



The Chinese Herbal Formula Ruyan Neixiao Cream Inhibits Angiogenesis of Precancerous Breast Lesions via Regulation of Ras/Raf/MEK/ERK Signaling Pathway

Integrative Cancer Therapies
Volume 21: 1–19
© The Author(s) 2022
Article reuse guidelines:
sagepub.com/journals-permissions
DOI: 10.1177/15347354211069397
journals.sagepub.com/home/ict


Shujun Lin, MD^{1*} , Xuefeng Jiang, MD^{1*}, Guijuan Zhang, MM^{2*}, Xinqin Xiao, MM¹, Xinyi Ma, MB³, Jieyan Wu, MM¹, Dan Qiu, MD¹, Xinyuan Li, MB⁴, Xianxin Yan, MD¹, and Min Ma, MD^{1,2}

Abstract

Ruyan Neixiao Cream (RUC) is a traditional Chinese herbal formula which can effectively inhibit the angiogenesis of breast precancerous lesions. In order to reveal the specific mechanism, we carried out experiments *in vitro* and *in vivo*. We found that the conditioned medium of MCF-10AT cells treated with RUC transdermal solution (RUCt) could significantly inhibit the proliferation, migration, invasion, tube formation of HUVECs and the capillary formation of rat aortic rings. RUCt may down-regulate the expression of VEGF, MMP2, and MMP9 in MCF-10AT medium by down-regulating miR-21 and up-regulating TIMP-3 and RECK. We further confirmed in rats that the microvascular density of precancerous lesions decreased significantly after external use of RUC, which may be related to the inhibition of Ras/Raf/MEK/ERK signaling pathway related proteins. Presumptively, RUC may inhibit the angiogenesis of breast precancerous lesions by inhibiting Ras/Raf/MEK/ERK signaling pathway, thus relieving the inhibition of miR-21 on TIMP-3 and RECK, then down-regulating the secretion of angiogenic factors.

Keywords

breast precancerous lesions, angiogenesis, Ras/Raf/MEK/ERK, miR-21, Ruyan Neixiao Cream(RUC)

Submitted March 25, 2021; revised November 10, 2021; accepted December 9, 2021

Introduction

Breast cancer is one of the most common cancers among women in the world (154/185), accounting for 25% of all cancers diagnosed in women.¹ There were 2.08 million new cases and 626 679 deaths in BC estimated by Global Cancer Statistics in 2018. The development of breast cancer is a continuous process, which goes through “usual ductal hyperplasia (UDH)-atypical ductal epithelial hyperplasia (ADH)-ductal carcinoma in situ (DCIS)-invasive breast cancer (IBC).”² WHO reported that lesions with the possibility of becoming malignant of more than 20% are classified as precancerous lesions, which appear before malignant tumors; some degree of atypical hyperplasia appears in morphology, but they do not have characteristic malignant changes.² The canceration rate of atypical hyperplasia of the breast is 4 times greater than other breast hyperplasia, and about 10% of atypical hyperplasia lesions will develop into breast cancer.³ Therefore, blocking development of breast cancer in precancerous stage is an important treatment strategy.

Breast cancer is a typical vascular-dependent tumor: it needs neovascularization when tumor grows to 1 to 2 mm^{3,4}. Numerous studies have shown that the carcinogenic mechanism of breast precancerous lesions is closely related to tumor angiogenesis, oncogene expression, endocrine

¹School of Traditional Chinese Medicine, Jinan University, Guangzhou, China

²The First Affiliated Hospital of Jinan University, Guangzhou, China

³Southern Medical University (No.3210090112), Guangzhou, China

⁴School of Medicine, Jinan University, Guangzhou, China

*These authors contributed equally to this work.

Corresponding Authors:

Min Ma, School of Traditional Chinese Medicine, Jinan University, No. 601, West Huang-pu Avenue, Guangzhou, Guangdong 510632, China. Emails: mamin020@163.com; tmamin@jnu.edu.cn

Xianxin Yan, School of Traditional Chinese Medicine, Jinan University, No. 601, West Huang-pu Avenue, Guangzhou, Guangdong 510632, China.

Email: yanxianxin@jnu.edu.cn.



disorders, and so on.² Studies have shown that with the process of breast cancer, the more serious the nature of breast cancer was, the higher the expression of VEGF, bFGF, and other angiogenic factors in serum and tissues, and the more neovascularization.^{5,6} Clinical studies have observed that atypical hyperplasia with high microvessel density (MVD) and high expression of VEGF, bFGF in serum and carcinoma in situ are high risk factors for breast cancer.⁷ Imaging study also showed that the blood flow signal of breast cancer tissue was significantly enhanced, angiogenesis was active, and the level of tumor angiogenesis activity could reflect the prognosis.⁸ Thus, angiogenesis is an important pathological change to reflect the malignant tendency of breast precancerous lesions. In breast cancer, Ras/Raf/MEK-ERK and other pathways are highly activated, and are of great significance in occurrence and development of breast cancer.⁹ It has been found that the Ras/Raf/MEK/ERK signaling node is not only plays a role in cell proliferation, apoptosis and invasion, but also is a regulatory center of various signaling pathways of angiogenesis.^{9,10} This signaling pathway coordinates many signals that promote or inhibit angiogenesis to determine the final state of neovascularization.⁹

For the treatment of breast precancerous lesions, current Western medicine methods are surgery and medicine.² Western medicine mainly includes tamoxifen (TAM), raloxifene (Ral), exemestane, anastrozole, targeted drugs, and some other drugs which need long term follow-up and more large-scale clinical trials to confirm their efficacy and safety in preventing and treating of breast precancerous lesions, such as aspirin, bisphosphonate, metformin, 27-hydroxycholesterol, tretinoin, fenretinide, vitamin D, and calcium. Although the above methods have certain effects on the treatment of breast precancerous lesions, they are expensive or have adverse reactions such as drug resistance.^{11,12} Recently, due to the increasing interest in traditional Chinese medicine anti-tumor effects, research work in this area is also increasing.¹³ Anti-tumor angiogenesis properties of traditional Chinese medicine are gradually becoming an important research direction.

According to the famous prescription of “Yin Du Nei Xiao San” in “Yao Lian Qi Mi,” Professor Ma Min obtained RUC, which is an effective traditional Chinese medicine for prevention and treatment of breast precancerous lesions. The preparation process and parameters of RUC has obtained a national invention patent (national invention certificate number: CN201110029344.1).¹⁴ RUC consists of 9 traditional Chinese herbs, including clove, rhubarb, frankincense, myrrh, borneol, rhizoma corydalis, cowherb seed, Rosae rugosae, and garden balsam stem. Previous studies have found that both in vitro and in vivo experiments of RUC and its drug monomer showed good inhibition of cell proliferation, cell cycle, cell invasion and tumorigenesis of breast precancerous lesions.^{15,16} Interestingly, we noticed that RUC can reduce the expression level of VEGF, FGF2

and other angiogenesis promoting factors in breast precancerous lesions.¹⁷ However, its regulation mechanism of angiogenesis is still unclear. Therefore, this study intends to verify the in vivo and in vitro experiments in order to study the effect of RUC on the Ras/Raf/MEK/ERK signaling pathway and angiogenesis in breast precancerous lesions.

Materials and Methods

Reagents

All herbs were provided by the First Affiliated Hospital of Jinan University (China). Blank matrix and RUC (1 g of high or low dose RUC respectively contained 4 g or 2 g herbal drugs) was prepared in the School of Traditional Chinese Medicine, Jinan University.¹⁴⁻¹⁶ The effective components and quality control of drugs have been analyzed by HPLC-MS in our previous studies.¹⁴ 7,12-dimethylbenz(a)anthracene (DMBA) was purchased from Tokyo Chemical Industry Co., Ltd (Tokyo, Japan). Tamoxifen was purchased from Chi-Fei Chemical Co., Ltd (Wuhan, China). The DMEM/F-12 medium, DMEM High Glucose medium, horse serum, fetal bovine serum (FBS) and rhEGF were purchased from Gibco BRL (Grand Island, NY, USA). Matrigel was purchased from BD Biosciences (San Jose, CA, USA). VEGF, MMP2, and MMP9 ELISA kits were purchased from Cusabio Biotech Co., Ltd (Wuhan, China). H-Ras, c-Raf, MEK, p-MEK, ERK, p-ERK, c-jun, and c-fos primary antibodies were purchased from Cell Signaling Techniques (Beverly, MA, USA). VEGF, MMP2, MMP9, CD34, and β -actin were purchased from Abcam (Cambridge, MA, USA).

Cell Culture and Transfection

We obtained the breast precancerous lesion cell line MCF-10AT from the American Karmanos Cancer Research Institute (KCI). We purchased human umbilical vein endothelial cells (HUVECs), MCF-10A and human mammary epithelial cells (HMEpiC) from ATCC. We cultured MCF-10A and MCF-10AT cells in DMEM/F-12(1:1) supplemented with 5% horse serum, 10 μ g/ml Insulin, 50 μ g/ml hydrocortisone, 20 ng/ml recombinant EGF, 100 U/ml penicillin, and 100 μ g/ml streptomycin. We cultured HUVECs and HMEpiC in DMEM medium (supplemented with 10% FBS, 100 U/ml Penicillin, and 100 μ g/ml Streptomycin). We cultured all cells in a 37°C constant incubator containing 5% CO₂, following standard protocols.

We transfected H-Ras siRNA (siH-Ras), miR-21-mimic and miR-21-inhibitor into cells using Lipofectamine 2000 (Invitrogen Life Technologies, Carlsbad, CA, USA) according to the manufacturer's protocol. We quantified transfection efficiency by counting green fluorescent protein (GFP)-positive cells 24 hours after transfection and found them to be about 60% to 70%.

Animal Studies

A total of 60 female Sprague-Dawley specific-pathogen-free rats (weight 160-180 g) were purchased from Jinan Pengyue Experimental Animal Breeding Co., Ltd (Shandong, China), Animal Certificate Number (Certified No. SCXK (Lu)2014-0007). All animals had free access to food and tap water. After adaptation for 1 week, we randomly divided rats into 6 groups according to their weight (8 per group): Normal group, Model group, Matrix group, TAM group, H-RUc group, and L-RUc group. All animal experiments were approved by the Laboratory Animal Ethics Committee of Jinan University (Ethics number: 2018319-136) (Guangzhou, China). All procedures were in line with the Statute on the Administration of Laboratory Animal approved by China's Council 1988.

As described previously,^{14,15} we combined DMBA with estrogen and progesterone to establish the breast precancerous lesion rat model. Then the RUc groups and TAM group were applied the ointment containing medicine on the rat's breast for treatment, while the matrix group was applied the medicine-free ointment and the model group was not applied with any ointment. At the 14th week, rats were sacrificed, the breast tissue samples were obtained and either stored at -80°C or fixed in 4% paraformaldehyde phosphate buffer for further examination.

Conditioned Medium Preparation

According to the experimental needs, the HEMpiC, MCF-10A, and MCF-10AT cells in logarithmic growth period were cultured in complete medium for 24 hours, then washed with PBS 3 times, adding new medium according to the groups. After 48 hours culture, we collected supernatant and centrifuged as conditioned medium (CM), stored at -80°C .

Cell Viability Assay

We used the MTT assay to measure cell viability. In short, we cultured cells in different CM for 48 hours. Then we added $20\ \mu\text{l}$ MTT to each well, further incubating them for 4 hours. We removed the supernatant, added $200\ \mu\text{l}$ DMSO and shook for 10 minutes. Finally, we detected the optical density (OD) value under 490 nm by a microplate reader (Biorad, CA, USA), and used the following formula to count the results of the viability assay:

$$\text{Cell survival rate} = \frac{\left(\frac{\text{experimental group} -}{\text{blank group OD}} \right)}{\left(\frac{\text{control group} -}{\text{blank group OD}} \right)} \times 100\%$$

Scratch Wound Healing Assay

HUVECs of logarithmic growth period were seeded in a 24-well plate at $1 \times 10^5/\text{mL}$ and cultured to 85% confluence. Then we scratched the cell monolayer with a pipette tip, and washed the well plate with PBS 3 times to remove the cell fragments produced by the scratches. Then, we added CM to the plate, measured the scratched widths of each group at 0 and 24 hours respectively, and analyzed the wound closure.

Invasion Assay

About 50 ml diluted Matrigel was spread evenly in the upper transwell chamber, which was placed for 30 minutes in 37°C constant incubator. HUVECs of logarithmic growth stage were collected, and added the CM to make the cell suspension. We added $100\ \mu\text{l}$ cell suspension to upper chamber, $500\ \mu\text{l}$ complete medium containing 10% FBS was added to the lower chamber, and it was cultured for 24 hours. Then the medium, Matrigel and removed the non-penetrative cells on the upper chamber. After fixation and staining, different visual fields were randomly selected to take photos under the microscope.

Tube Formation Assay

As described in Zhang et al,¹⁸ HUVECs of logarithmic growth period were collected, and CM was added. We seeded the cells in a 48-well plate which was coated with Matrigel. After 6 hours of cell culturing in the incubator, we observed the formation of lumen structure under inverted microscope, and 10 fields of vision were randomly selected to count and analyze the lumen structure.

Chorioallantoic Membrane Vascular Assay (CAMVA)

A total of 40 fertilized chicken eggs (3-day-old) were incubated at 37.8°C and 60% humidity for 10 days. We opened a small window at the top of the air chamber and removed the shell membrane, and dripped sterile physiological saline on the shell membrane. We washed out the air in the air chamber, causing negative pressure in the air chamber and forming an artificial air chamber. Finally, $100\ \mu\text{l}$ culture medium was added to each group's allantoic membrane under aseptic conditions, sealed with aseptic adhesive tape, and incubated at 37.8°C and 60% humidity. After 5 days of incubation, we collected allantoic membrane, and observed the CAM angiogenesis under microscope and counted.

Rat Aortic Ring Assay

As described in Zhang et al,¹⁸ the aorta separated from the thoracic region of SD rats was cleaned, the fat around the

Table 1. The Primer Sequence of Genes.

Gens	Species	Forward primer (5'→3')	Reverse primer (5'→3')
TIMP-3	Homo	CTATCGGTATCACCTGGGTTGTA	ATGCAGGCGTAGTGTTTGGGA
RECK	Homo	AGCACATAATGGGGCAACAAGC	GGCACAATGGTGAGACCTACA
GAPDH	Homo	GGACCTGACCTGCCGTCTAG	GTAGCCCAGGATGCCCTTGA
TIMP-3	Rat	CCCTTTGGCACTCTGGTCTA	TGTCAGCAGGTAAGTGGTATTTGT
RECK	Rat	GTGGCAGTGGATTACTATGGG	CTGGTGGAAATGATGGGTTTG
GAPDH	Rat	GCCTTCCGTGTTCCCTACC	CCTGCTTACCACCTTCTT

blood vessel and small branches of microvasculature was removed and the aorta then was cut into 1 to 1.5 mm rings. After starvation overnight in a 37°C incubator, we randomly placed the arterial rings at the bottom of the 48-well plate coated with Matrigel, and another 100 µl Matrigel was drawn to cover the arterial rings. After coagulation, we added 500 µl conditioned medium to each well for further culture, and the growth state of the aortic ring was observed for numbers and branches of neovascularization with inverted fluorescence microscope (Carl Zeiss, Germany). The number of neovascularizations in each well was recorded and analyzed on the 6th day.

Enzyme-linked Immunosorbent Assay (ELISA)

The expression levels of VEGF, MMP-2, and MMP-9 in CM were detected according to the instructions of the ELISA kit. The quantitative determination of concentration was carried out in accordance with the manufacturer's procedures and repeated 3 times.

RT-PCR

Total RNA was isolated from the cells using the RNAiso Plus and then reverse-transcribed using iScript cDNA Synthesis Kit according to the manufacturer's instructions. An equal volume of cDNA was then used for RT-PCR using the SYBR-Green Quantitative PCR kit and the CFX96 Touch Real-Time PCR Detection System (Bio-Rad, USA). RT-PCR primers are showed in Table 1. The relative quantification results were calculated using the formula $2^{-\Delta\Delta Ct}$.

Western Blot

The total protein of each group was extracted from cells and rat tissue, and the BCA protein assay kit was used to analyze the protein concentration. The total protein was separated by SDS-PAGE gel (P0012AC, Beyotime Biotechnology, China) was electrophoretically transferred to PVDF membranes (#88520, Thermo Fisher, USA) and sealed for 1 hour, and incubated overnight at 4°C with the following primary antibodies: H-Ras, c-Raf, p-MEK, p-ERK, RECK, TIMP3, VEGF, MMP2, and MMP9. After

washing the membrane with TBST, it was incubated with the corresponding Goat anti-rabbit IgG (H + L) secondary antibody of Goat anti-mouse IgG (H + L) secondary antibody for 1 hour. Finally, protein bands were electrochemiluminescence kit and visualized in ChemiDoc Imaging System (BIO-RAD, USA), Image J software was used to analyze the gray scale quantitation of Western blots.

Luciferase Reporter Assay

The wild-type (WT) or mutant (MUT) type of TIMP-3 and RECK 3'-UTR were synthesized and fused to a luciferase reporter vector psiCHECK-2 (Promega, Madison, WI, USA). MCF-10AT cells were co-transfected with reporter vector and miR-21 mimics or negative control. After transfection for 24 hours, the relative luciferase activity was measured using a Dual-Luciferase Reporter Assay System according to the manufacturer's instructions.

HE Staining

The breast tissue of rats was fixed in 4% paraformaldehyde phosphate buffer for 24 hours. After dehydration, it was embedded in paraffin and cut into sections with thickness of 6 µm continuously. After HE staining, the morphological changes of mammary tissue of rats were observed under light microscope (Nikon, Japan) and the images were collected for analysis.

Immunohistochemistry Assay

The sections were dewaxed and hydrated, and endogenous peroxidase was blocked with hydrogen peroxide. Then antigen was retrieved by citrate buffer. After that, the slides were incubated with primary and secondary antibodies, used DAB staining, counterstained with hematoxylin buffer and sealing. Finally, the expression of CD34 in rat breast tissue was observed under Olympus BX53 microscope (Japan) and analyzed with Image J software.

Statistical Analysis

Statistical analysis was performed using SPSS 21.0 software. Data are presented as mean ± SD. One-way ANOVA

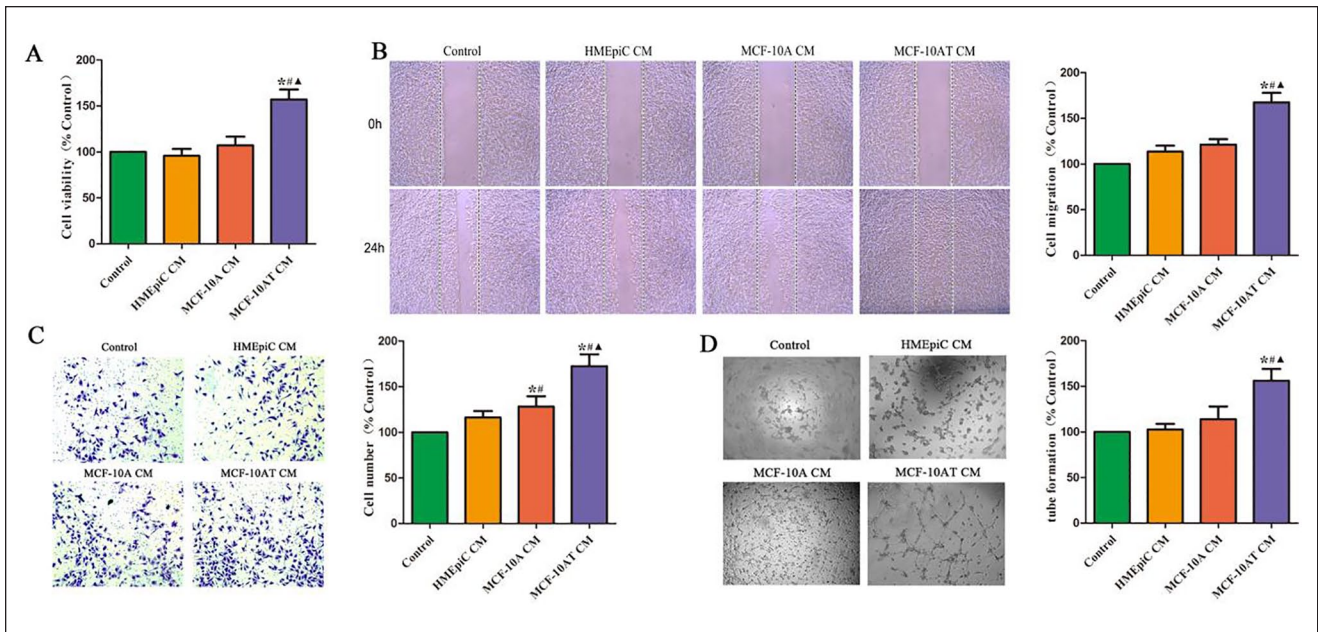


Figure 1. Effect of different cells' CM on the proliferation, migration, invasion, and generation of angiogenesis of HUVECs. (A) The effect of CM of different cells on the cell viability of HUVECs was analyzed by MTT assay. (B) The effect of different cells' CM on the migration of HUVECs was analyzed by scratch wound healing assay. (C) The effect of different cells' CM on the invasion of HUVECs was analyzed by transwell assay. (D) The ability of HUVECs to generate angiogenesis in vitro was analyzed by tube formation. * $P < .05$ versus Control. # $P < .05$ versus HMEpiC CM. $\Delta P < .05$ versus MCF-10A CM.

and Student-Newman-Keuls (*S-N-K*) method was using to compare the difference in groups. When variance was uneven, Tamhane's T2 method was used. $P < .05$ was considered to be statistically significant.

Results

The CM of MCF-10AT Cells Promoted the Proliferation of HUVECs

MTT assay was performed to determine the viability of HUVECs exposed to the CM of HMEpiC, MCF-10A, and MCF-10AT cells. We found that there was no significant difference in the viability of HUVECs in the CM of HMEpiC and MCF-10A cells (Figure 1A). And the CM of MCF-10AT cells significantly promoted the proliferation of HUVECs, compared to the CM of HMEpiC or MCF-10A cells.

The CM of MCF-10AT Cells Enhanced the Migration, Invasion, and Tube Formation of HUVECs

The experiments of migration ability of endothelial cells included scratch wound healing assay and transwell invasion assay. As shown in Figure 1B to D, the migration, invasion, and tube formation of HUVECs in control group, HMEpiC group and MCF-10A group showed no difference. Compared with the control group, the migration of HUVECs in MCF-10AT group was significantly enhanced. Moreover,

the invasion of HUVECs in MCF-10A and MCF-10AT groups also was significantly promoted. Additionally, compared with the control group, the formation of HUVECs tube-like structure in MCF-10AT group was promoted.

The CM of MCF-10AT Cells Promoted the Germination of Microvasculature in Chorioallantoic Membrane Vascular and Rat Aortic Ring

The effect of the CM of HMEpiC, MCF-10A, and MCF-10AT cells on the germination of microvasculature in vivo was detected by using the chorioallantoic membrane vascular and rat aortic ring. As shown in Figure 2, the microvessels around the rat aortic rings in MCF-10AT group were significantly increased versus those in control group. Meanwhile, compared with control group, the CM of MCF-10AT group significantly promoted the density of CAM blood vessel plexus. However, there was no difference in the germination of microvasculature between control group, HMEpiC group and MCF-10A group.

The Expression Levels of VEGF, MMP2, and MMP9 in HMEpiC, MCF-10A, and MCF-10AT Cells

The expression levels of VEGF, MMP2, and MMP9 were examined by ELISA in the CM of HMEpiC, MCF-10A, and

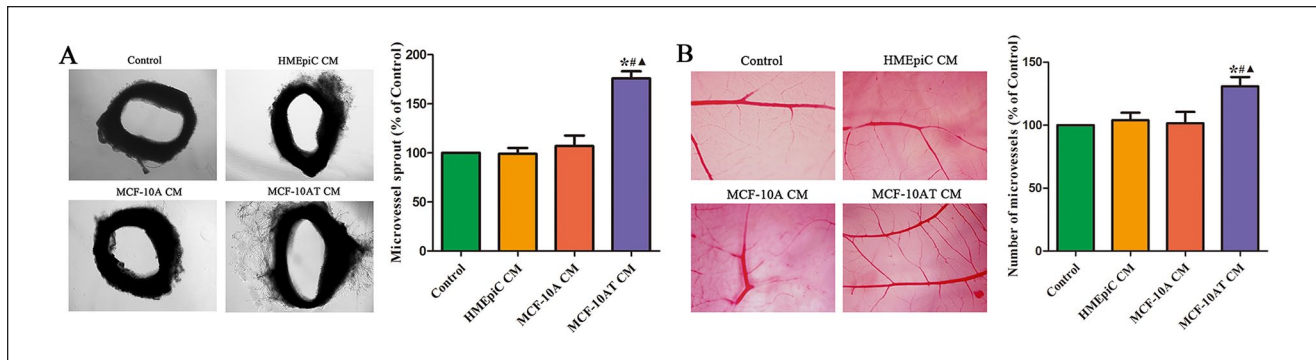


Figure 2. Effect of different cells CM on the angiogenesis in vitro. (A) The effect of different cells' CM on the formation of microvessel sprouting from rat aortic rings. (B) Effect of different cells' CM in angiogenesis of embryonic CAM. Data are shown as the mean \pm SD.

* $P < .05$ versus Control. # $P < .05$ versus HMEpic CM. $\Delta P < .05$ versus MCF-10A CM.

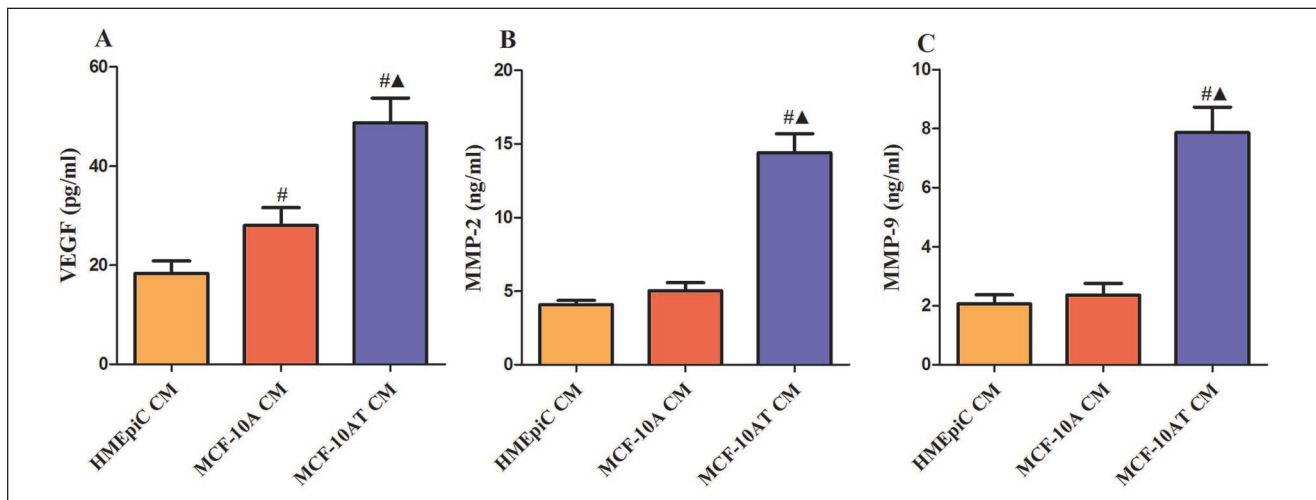


Figure 3. The expression levels of VEGF, MMP2, and MMP9 in HMEpic, MCF-10A, and MCF-10AT cells. (A) VEGF, (B) MMP2, (C) MMP9, the levels were tested from different cells' CM. Data are representative results of 3 independent experiments.

$P < .05$ versus HMEpic CM. $\Delta P < .05$ versus MCF-10A CM.

MCF-10AT cells. As shown in Figure 3, compared with the CM of HMEpic or MCF-10A cells, the expression of VEGF, MMP2, and MMP9 were significantly increased in the CM of MCF-10AT cells. Then, we used Western blot to verify their protein expression levels in cells. The results shown that the protein expressions of VEGF, MMP2, and MMP9 were significantly up-regulated in the MCF-10AT cells, compared with HMEpic or MCF-10A cells (Figure 4).

Effect of RUt on the Viability of HUVECs and MCF-10AT cells

To determine the dose of RUt in HUVECs and MCF-10AT cells, we measured the cell viability by MTT assay with different concentrations of RUt (0.2%, 0.4%, 0.8%, 1.6%, 2.4%, 3.2%, 4.8%, 6.4%) for 48 hours. As shown in Figure 5, RUt

could significantly inhibit the proliferation of MCF-10AT cells in a dose-dependent manner. The minimum effective concentration of RUt on MCF-10AT cells was 0.4%, and the 50% inhibitory concentration (IC₅₀) of RUt was about 1.58%. However, the minimum effective concentration of HUVECs was 3.2% and the IC₅₀ was 7.93% for RUt. This result indicated that low doses of the RUt may first affect MCF-10AT cells rather than HUVECs.

RUt Suppressed the Expression of H-Ras and c-Raf in MCF-10AT Cells

In order to investigate the regulation of Ras signaling pathway on angiogenesis, we carried out protein detection. The results of Western blot showed that the protein expressions of H-Ras and c-Raf were significantly decreased in the

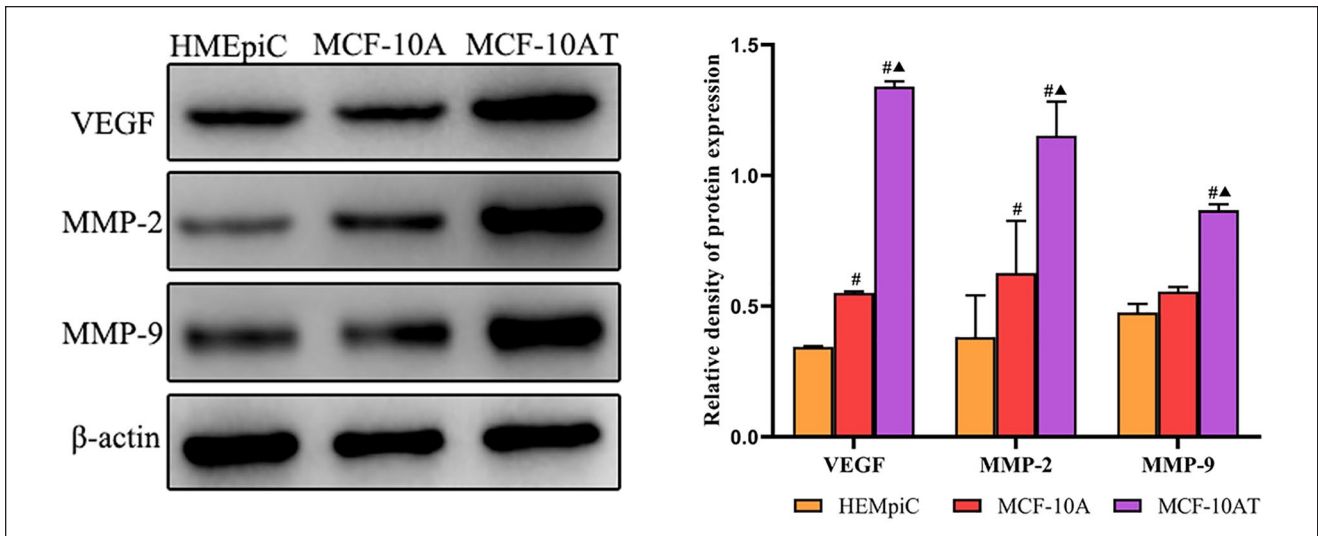


Figure 4. The protein expression levels of VEGF, MMP2 and MMP9 in cells. Data are representative results of 3 independent experiments.

$P < .05$ versus HMEpiC. ▲ $P < .05$ versus MCF-10A.

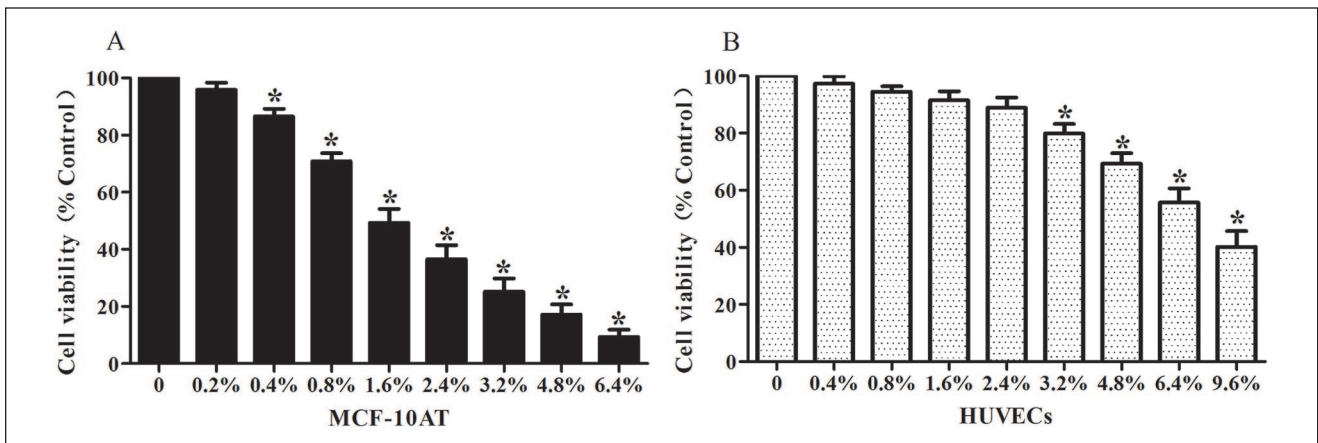


Figure 5. Effect of RUt on the cell viability of MCF-10AT cells and HUVECs. (A) MCF-10AT cells were treated with increasing doses of Rut for 48 hours incubation. (B) HUVECs cells were treated with increasing doses of Rut for 48 hours incubation. Then the cell viability was determined by the MTT assay. The data of cell viability are shown as mean \pm SD, and the no RUt treatment was used as a control group.

* $P < .05$ versus 0 hour.

TAM and different doses of RUt treated groups, and RUt had a dose-dependent effect (Figure 6). Among them, the inhibition of H-Ras and c-Raf protein expression was most significant in the 2.4% concentration of RUt.

Effect of RUt on miR-21, TIMP-3, and RECK in MCF-10AT Cells

Then, we measured the expression of miR-21, TIMP-3, and RECK mRNA in MCF-10AT cells after RUt treatment. The miR-21, TIMP-3, and RECK mRNA levels were not altered by vehicle in MCF-10AT cells (Figure 7). However,

miR-21 was significantly decreased, while TIMP-3 and RECK mRNA were increased in the TAM and different doses of RUt treated groups. Additionally, the 2.4% concentration of RUt had the most significant regulatory effect, so the 2.4% concentration was selected for subsequent experiments.

MiR-21 Targeted 3'UTR of TIMP3 and RECK mRNA to Suppress its Protein Translation

MiR-21 level was negatively associated with TIMP3 and RECK mRNA expression in MCF-10AT cells. According to

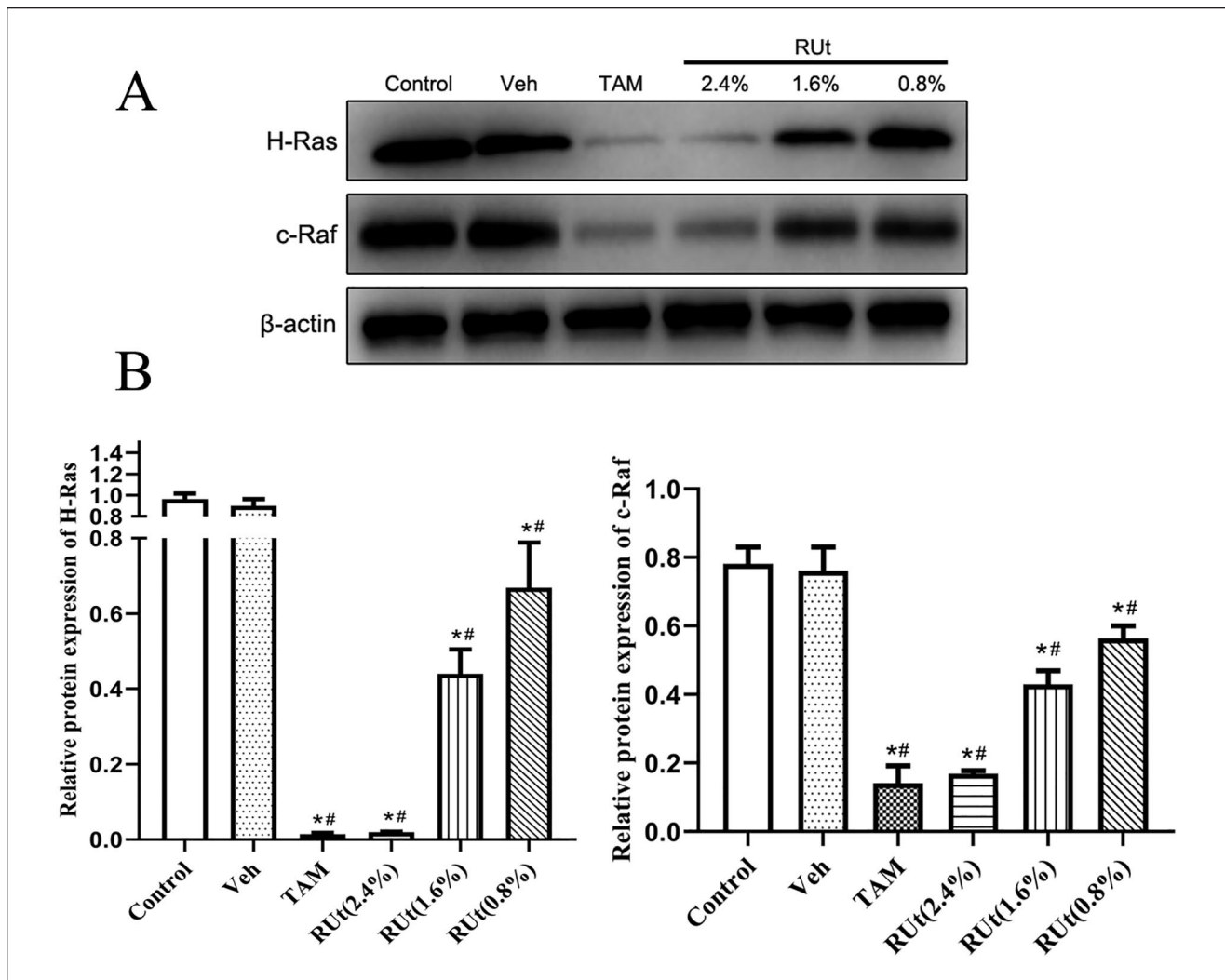


Figure 6. Effect of RUt on the expression of H-Ras and c-Raf in MCF-10AT. MCF-10AT were treated with different medicines or different concentrations for 48 hours. (A) Representative Western blot images of H-Ras and c-Raf in MCF-10AT cells. (B) The quantification of H-Ras and c-Raf protein levels. Data are shown as the mean \pm SD.

* $P < .05$ versus Control. # $P < .05$ versus vehicle.

TargetScan (<http://www.targetscan.org/mamm>), miRTarBase (<http://mirtarbase.mbc.nctu.edu.tw/php/index.php>), and miRDB (<http://mirdb.org/>) database prediction results, TIMP3 and RECK mRNA are potential targets of miR-21 in breast tumor. The binding sites between miR-21 and TIMP3, RECK are shown in Figure 8A. The dual-luciferase reporter assay indicated that miR-21 mimics could impair the luciferase activity of the WT TIMP3 and RECK, but not of the MUT TIMP3 and RECK (Figure 8B). In addition, the results of Western blot showed that the protein expression of TIMP3 and RECK increased in MCF-10AT cells transfected with miR-21 inhibitor compared with transfected with NC, indicating that TIMP3 and RECK are targets of miR-21 in MCF-10AT cells (Figure 8C).

The CM of MCF-10AT Cells After RUT Treatment Inhibited the Proliferation, Migration, Invasion, and Tube Formation of HUVECs

It is worth noting that the proliferation of HUVECs was inhibited in the CM of MCF-10AT cells after treating with RUt or TAM (Figure 9). Meanwhile, the migration, invasion and tube formation of HUVECs were reduced in the CM of MCF-10AT cells, which were treated with RUt or TAM, as shown in Figure 9B to D. We transfected siH-Ras into MCF-10AT cells to silence H-Ras expression. The results showed that the inhibition of RUt on the HUVECs was reversed.

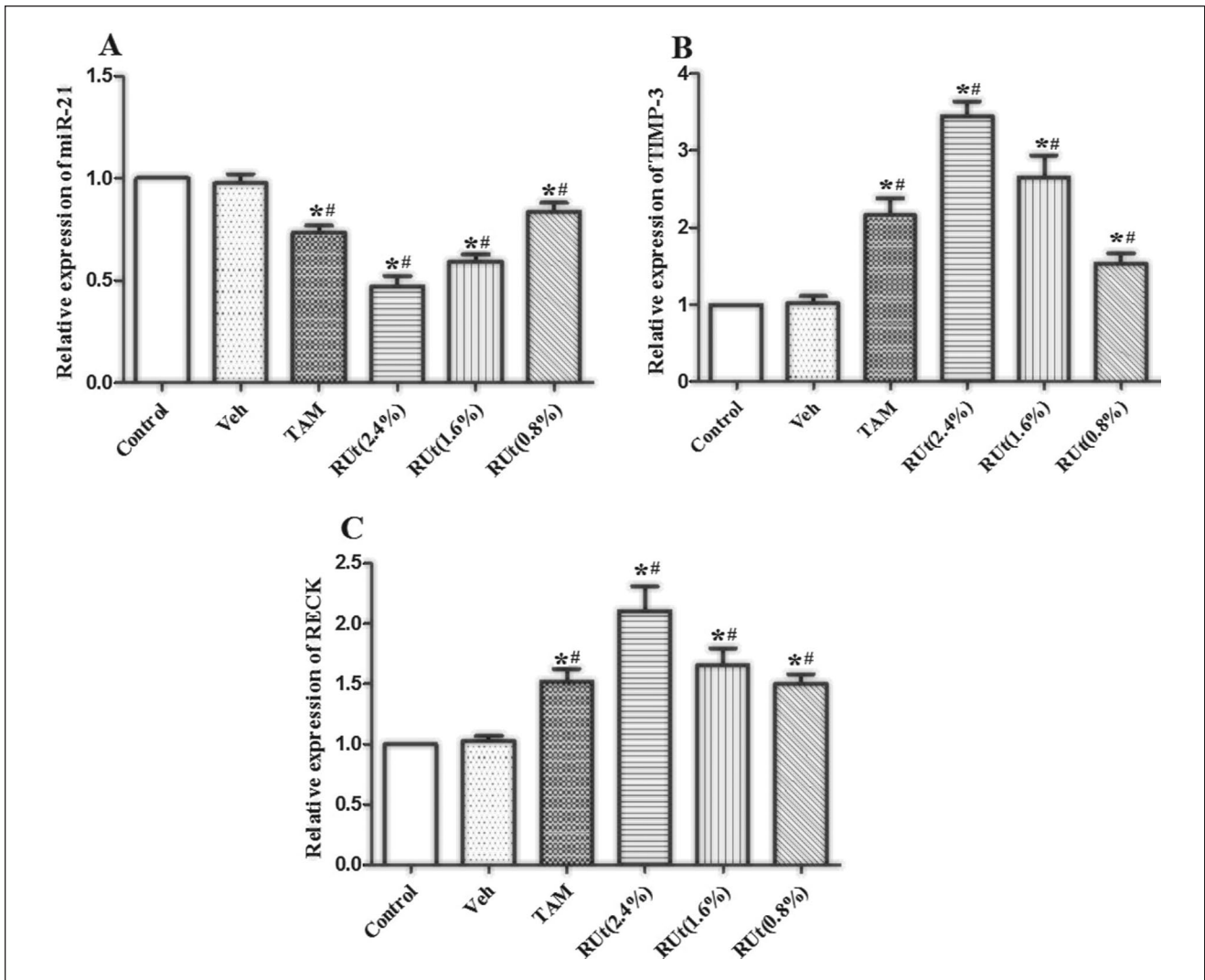


Figure 7. Effect of RUt on the expression of angiogenesis-associated genes miRNA21, TIMP-3, and RECK in MCF-10AT cells. (A) miRNA-21, (B) TIMP-3, (C) RECK. RT-PCR was used to analyze the expression levels of mRNA in MCF-10AT cells. Data are representative results of 3 independent experiments.

* $P < .05$ versus Control. # $P < .05$ versus Veh.

The CM of MCF-10AT Cells After RUT Treatment Reduced the Germination of Microvasculature in Rat Aortic Ring

As shown in Figure 10, the microvessels around the rat aortic rings in the CM of the RUt group and TAM group were significantly less than those in the Veh group. Meanwhile, there was no significant difference in the Veh group and the MCF-10AT-CM RUt+siH-Ras group.

RUt Down-Regulated VEGF, MMP2, and MMP9 in the CM of MCF-10AT Cells

As shown in Figure 11, the expressions of VEGF, MMP2, and MMP9 in the CM of MCF-10AT cells of RUt group and

TAM group were significantly reduced, while silenced H-Ras could restore inhibitory effect of VEGF, MMP2, and MMP9 by RUt.

Effect of RUt on the Key Protein Expression of Ras/Raf/MEK/ERK Signaling Pathway in MCF-10AT Cells

Furthermore, to explore the effect of RUt on the signal transduction pathways involving Ras/Raf/MEK/ERK, we used Western blot. The results showed that the expressions of H-Ras, c-Raf, p-MEK, p-ERK, c-jun, and c-fos were decreased significantly in the RUt group and TAM group (Figure 12). When siH-Ras was transfected into MCF-10AT cells to silence H-Ras expression, the regulatory effect of

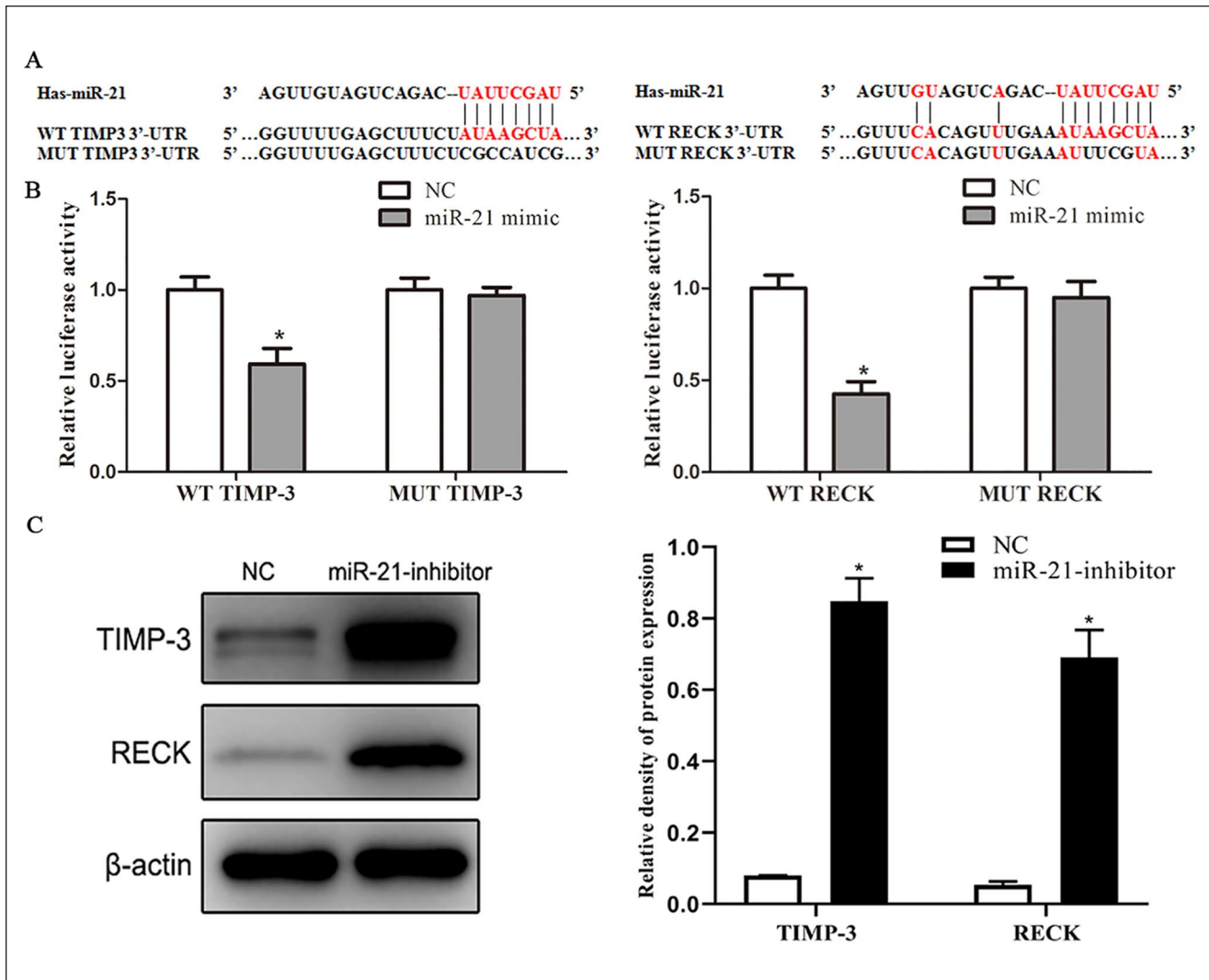


Figure 8. MiR-21 targeted 3'UTR of TIMP3 and RECK mRNA to suppress its protein translation. (A) The binding sites between miR-21 and TIMP3, RECK. (B) The relative luciferase activity of WT TIMP-3, MUT TIMP-3, WT RECK, and MUT RECK were measured in NC group and miR-21 mimic group by a Dual-Luciferase Reporter Assay System. (C) The protein expression levels of TIMP-3 and RECK in NC group and miR-21 inhibitor group were detected by Western blot. Data are shown as the mean \pm SD.

* $p < .05$ versus NC.

RUt on the key protein expression of the Ras/Raf/MEK/ERK signaling pathway in MCF-10AT cells disappeared.

RUt Regulated Angiogenesis-Associated Protein in MCF-10AT Cells

Furthermore, the protein expression of VEGF, MMP-2, and MMP-9 were down-regulated, while RECK and TIMP-3 were up-regulated in MCF-10AT cells by treating with RUt or TAM (Figure 13). The regulatory effect of angiogenesis-associated protein induced by RUt was restored by siRNA mediated silencing of H-Ras.

The Pathological Changes in Breast Tissue of Breast Precancerous Lesions Rats

In order to further verify the inference of the cell experiments, we carried out experiments in vivo. The animal model was established by DMBA combined with estrogen and progestin induction in SD female rats, and TAM was used as the positive control. The pathological morphological characteristics showed that there was no precancerous lesion or invasive cancer in the Normal group. However, varying degrees of precancerous lesions and invasive carcinoma were found in the breast tissues of the Model group,

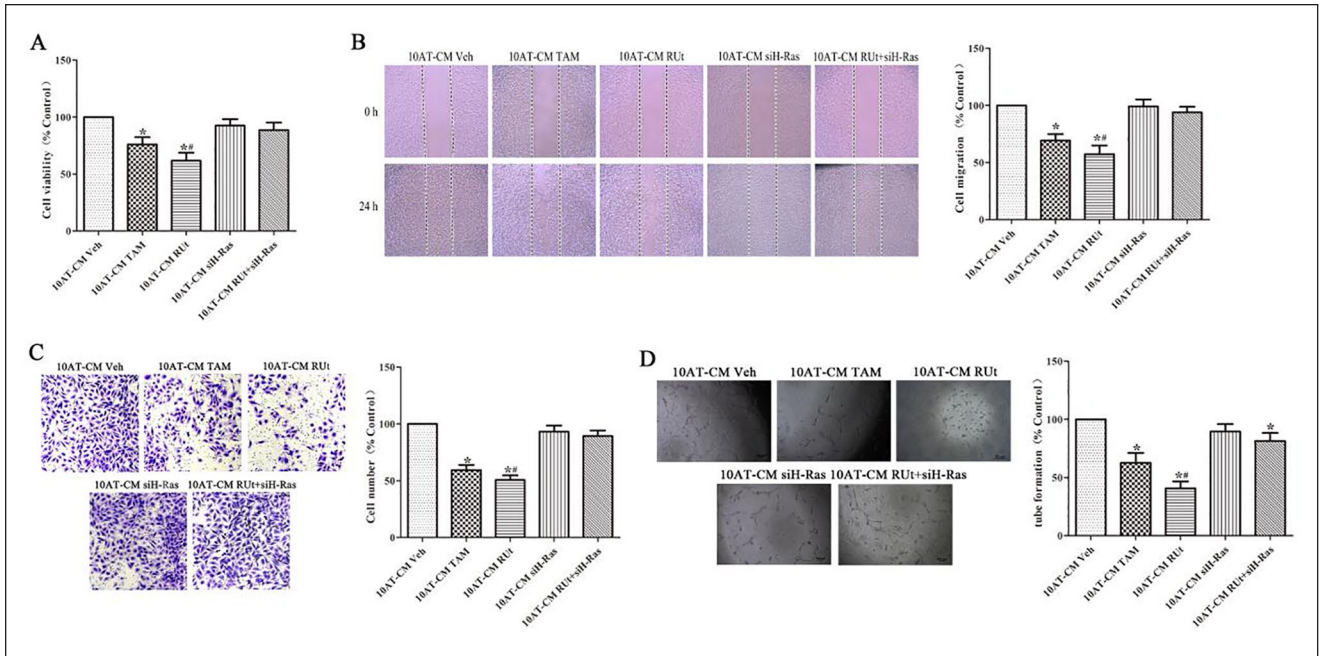


Figure 9. Effect of the CM of MCF-10AT cells after different treatment on the proliferation, migration, invasion and tube formation of HUVECs. (A) The effect of the different treatments' CM on the cell viability of HUVECs was analyzed by MTT assay. (B) The effect of the different treatments' CM on the migration of HUVECs was analyzed by Scratch wound healing assay. (C) The effect of the different treatments' CM on the invasion of HUVECs was analyzed by Transwell assay. (D) The ability of HUVECs to generate angiogenesis in vitro was analyzed by tube formation. * $P < .05$ versus 10AT-CM Veh. ** $P < .05$ versus 10AT-CM RUt+siH-Ras.

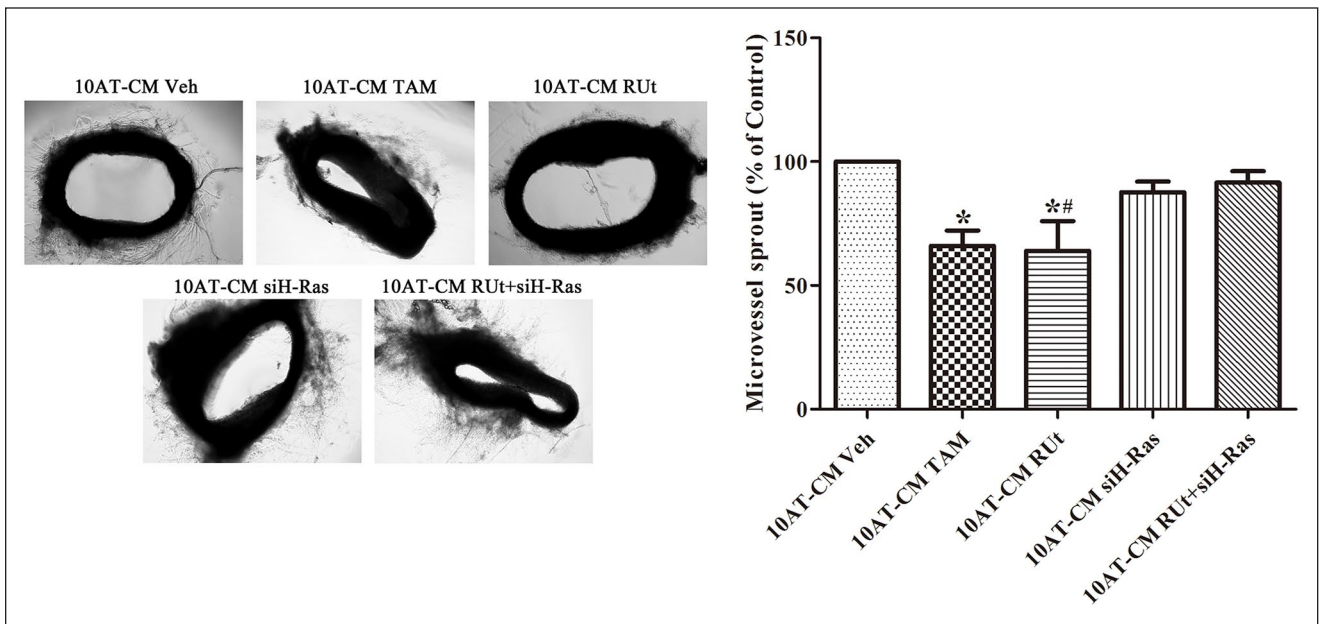


Figure 10. Effect of RUt on the formation of microvessel sprouting from rat aortic rings. Data are shown as the mean \pm SD. * $P < .05$ versus 10AT-CM Veh. ** $P < .05$ versus 10AT-CM RUt+siH-Ras.

Matrix group, TAM, H-RUC, and L-RUC groups (Figure 14). The mammary tissues in the Model group and Matrix group showed atypical ductal or lobular hyperplasia of type III.

The results suggested that DMBA combined with estrogen and progesterin could successfully replicate breast precancerous lesions rat model. What is interesting is that the

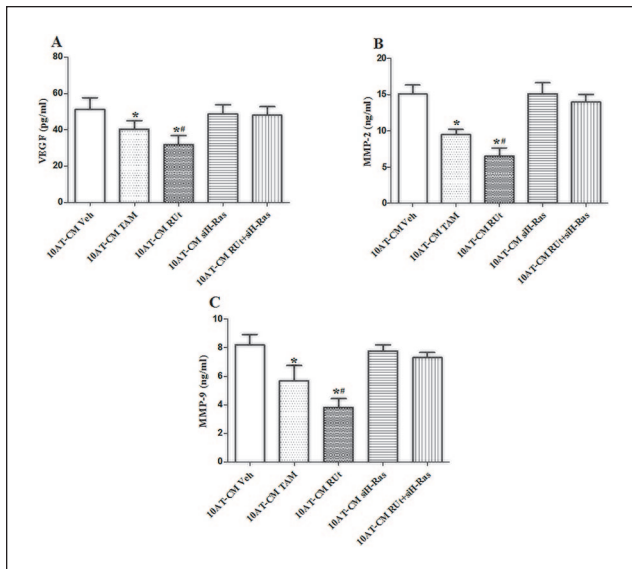


Figure 11. Effect of RUt on the expression levels of VEGF, MMP2, and MMP9 in MCF-10AT cells. (A) VEGF, (B) MMP2, (C) MMP9; the expression levels were tested by ELISA. Data are representative results of 3 independent experiments. * $P < .05$ versus I0AT-CM Veh. # $P < .05$ versus I0AT-CM+siH-Ras.

incidence of precancerous lesions and invasive carcinomas were decreased in the TAM, H-RUC and L-RUC groups; the occurrence rates of precancerous lesions were respectively decreased by 55.8%, 44.2%, 26.7% (Table 2). This showed that TAM and RUC could alleviate the pathological changes of breast tissue in a rat model with breast precancerous lesions.

Effect of RUC on MVD in Breast Tissue of Breast Precancerous Lesions Rats

To verify the inhibitory effect of RUC on angiogenesis in vivo, we used immunohistochemistry (IHC) to detect the microvascular density (MVD) marker CD34 of rat breast tissue. The result showed that the expression of CD34 was increased in the Model group and Matrix group, as shown in Figure 15. But the expression of CD34 in the TAM, H-RUC, and L-RUC groups were significantly decreased, indicating that RUC reduced the MVD of rat model breast tissue.

Effect of RUC on the Expression of Ras/Raf/MEK/ERK Signaling Pathway Key Protein in Breast Tissue of Breast Precancerous Lesions Rats

In order to verify the intervention mechanism of RUC on the precancerous breast lesions, SD rats were smeared with different concentrations of RUC every day for 14 weeks.

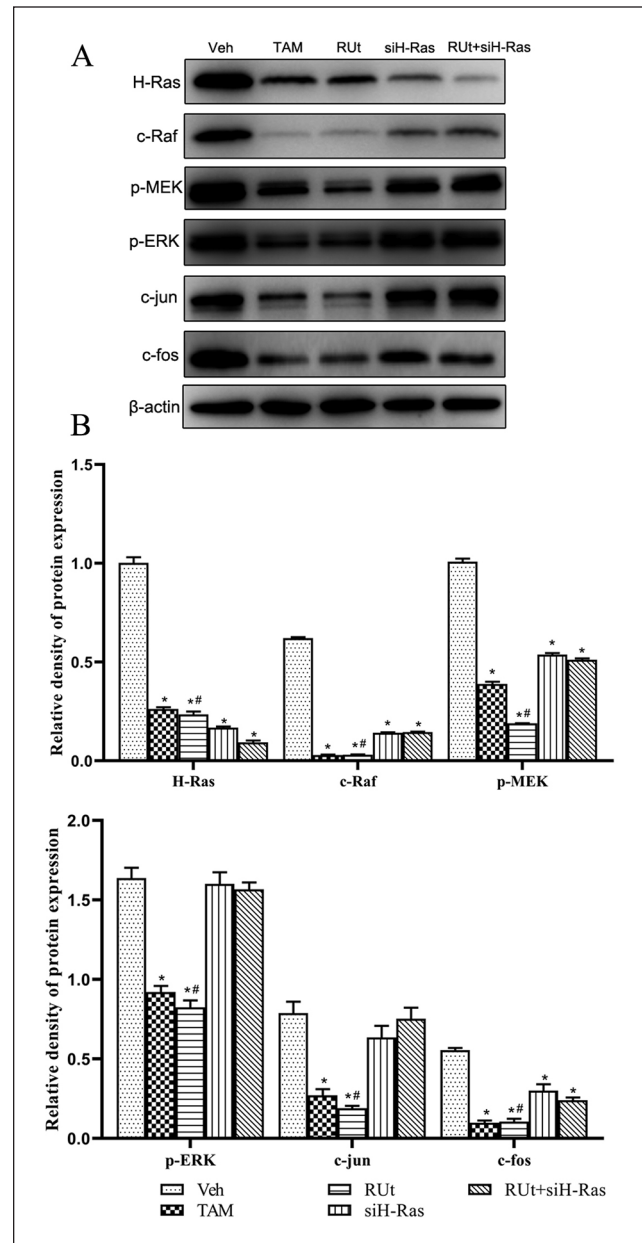


Figure 12. Effect of RUt on the regulation of the Ras/Raf/MEK/ERK signaling pathway. MCF-10AT cells were treated with different treatment for 48 hours, and Western blot was used to analyze the regulation of RUt on the Ras/Raf/MEK/ERK signaling pathway related proteins. (A) Representative Western blot images. (B) The quantification of protein levels. * $P < .05$ versus I0AT Veh. # $P < .05$ versus I0AT RUt+siH-Ras.

Western blot results showed that the expression of Ras/Raf/MEK/ERK signaling pathway key protein of H-Ras, c-Raf, p-MEK, p-ERK, c-jun, and c-fos were significantly increased in the Model group and Matrix group compared with the Normal group (Figure 16). Nevertheless, the protein expressions of H-Ras, c-Raf, p-MEK, p-ERK, c-jun,

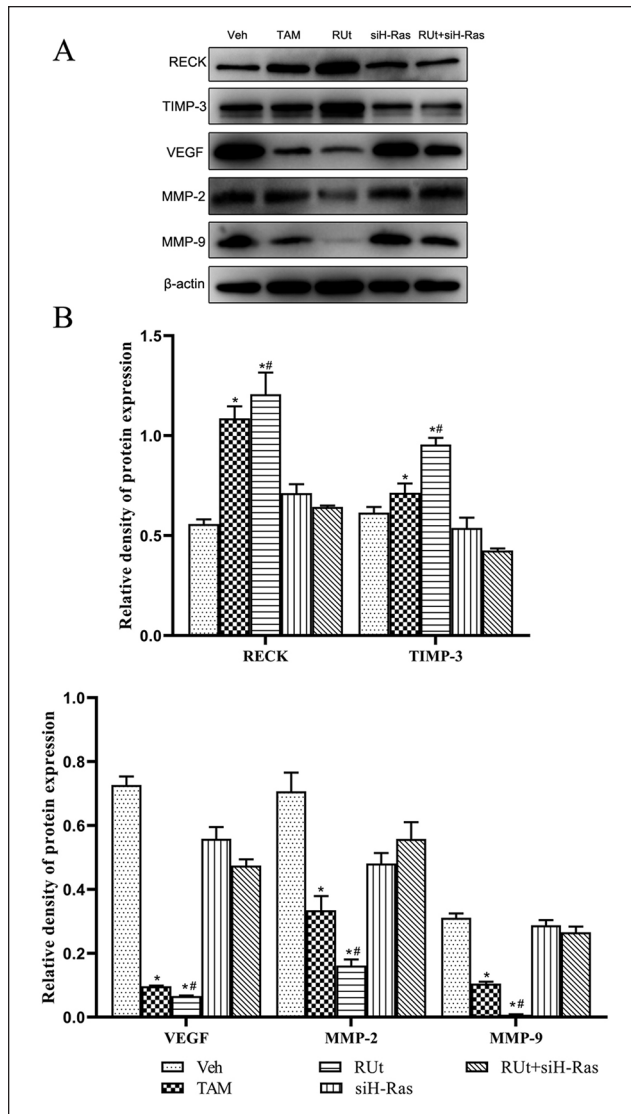


Figure 13. Effect of RUt on the regulation of the angiogenesis related proteins. MCF-10AT cells were treated with different treatments for 48 hours, and Western blotting was used to analyze the related proteins.

* $P < .05$ versus 10AT Veh. # $P < .05$ versus 10AT RUt+siH-Ras.

and c-fos were decreased in the TAM, RUc (High or Low dose) groups.

Effect of RUc on the Expression of miR-21, TIMP-3, and RECK mRNA in Breast Tissue of Rats With Breast Precancerous Lesions

RT-PCR results showed that the expression of miR-21 was increased, while TIMP-3 and RECK were decreased in the Model group and Matrix group compared with the Normal group (Figure 17). At the same time, the expression of

miR-21 was decreased, and TIMP-3 and RECK were increased in the TAM group and different doses of RUc groups.

Effect of RUc on Expression of Angiogenesis-Associated Protein in Breast Tissue of Rats With Breast Precancerous Lesions

As shown in Figure 18, the protein expression levels of VEGF, MMP2, and MMP9 in breast tissue of the Model and Matrix groups were significantly increased compared with the Normal group. Meanwhile, the expressions of RECK and TIMP3 were reduced. Additionally, the expression of VEGF, MMP2, and MMP9 proteins were significantly decreased, while TIMP-3 and RECK were increased in TAM and different doses of RUc groups.

Discussion

According to the American Cancer Society's 2018 estimate, there were 266 120 new cases of DCIS and 63 960 lobular carcinoma in situ (LCIS), respectively. And it alone was anticipated to account for 30% of all new cancer diagnoses in females.¹⁹ Hoogerbrugget's prospective study found 37% atypical lobular hyperplasia, 39% atypical ductal hyperplasia, 25% lobular carcinoma-in-situ, and 15% ductal carcinoma-in-situ in the susceptible population of breast cancer.²⁰ The precancerous breast lesions, the essential stage of breast cancer progression, could be blocked or reversed via specific drug intervention.²¹

MCF-10A cells are derived from an American female patient with breast fibrocystic lesion, which are spontaneously immortalized, non-tumorigenic, "normal" breast epithelial cells.²² Dr. Miller et al^{23,24} established MCF-10AT cell model of breast precancerous lesions by transfection of MCF-10A cells with t24c-h-ras mutation in 1996. MCF-10AT cells have uncertain proliferative ability, showing a wide range of structures from normal to atypical hyperplasia and carcinoma in situ. After inoculating the cells into nude mice, about 25% of transplanted tumors can develop into infiltrating cancer in 50 days to 2 years, which natural evolution process is very similar to that of human breast cancer. Therefore, we used MCF-10AT cells as a cell model of breast precancerous lesions in vitro.

Ras protein is a kind of small molecule GTP enzyme protein, which is the same as Ran, RAB, Rho, ARF/Sara, and other subtypes, all of which are members of Ras protein superfamily. Ras protein is involved in cell proliferation and differentiation, and is the main regulator of the MAPK signaling pathway.²⁵ When the extracellular signal is transmitted to the cell membrane, the ligands and specific receptors bind to form dimers, which activate their own tyrosine kinases, and Ras binds to GTP to activate Ras protein.

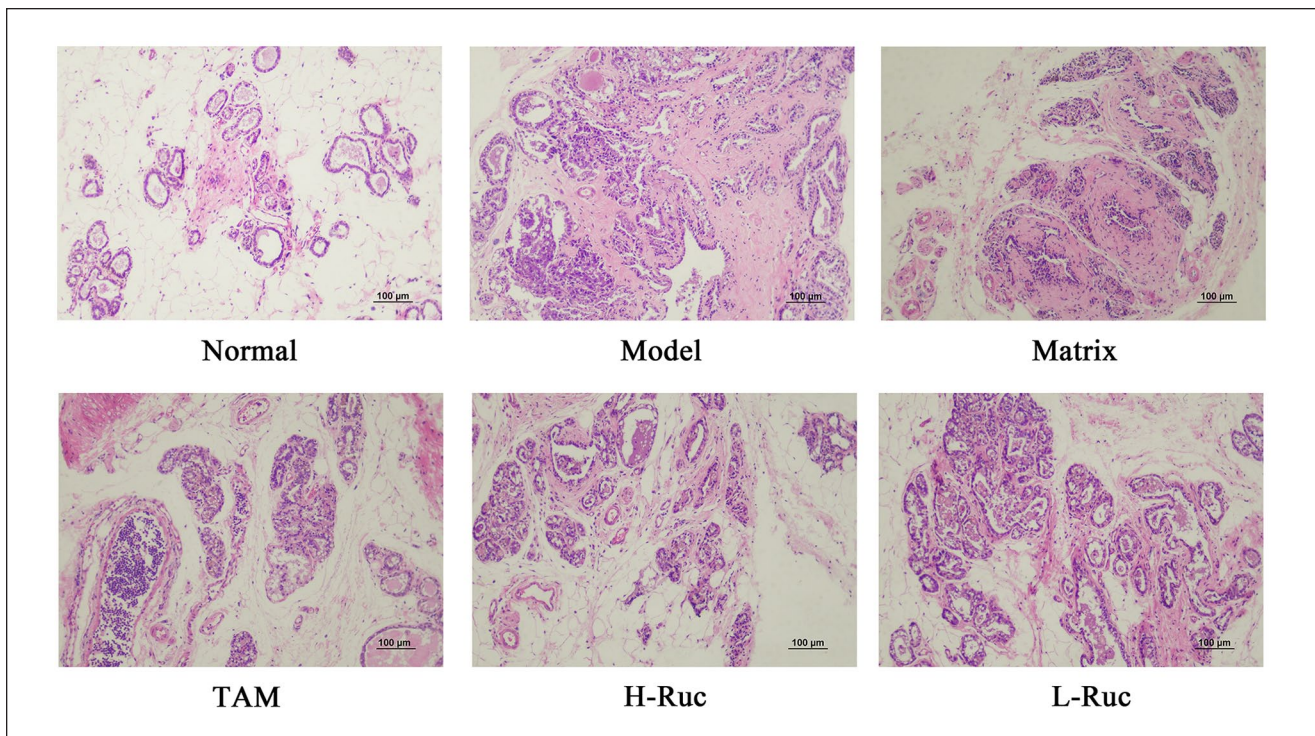


Figure 14. HE stained images revealed the pathological changes of breast precancerous lesions rats ($\times 200$ magnification. Scale bars: 100 μm).

Table 2. The Pathological Changes of Mammary Gland Tissue in Rats in Each Treatment Group.

Groups	Breast number	No hyperplasia	General hyperplasia	Precancerous lesions	Invasive carcinoma
Normal	120	113	7	0	0
Model	120	0	12	102	6
Matrix	120	4	19	98	3
TAM	120	19	46	53	2
H-RUc	120	20	48	49	3
L-RUc	120	16	31	70	3

By Kruskal-Wallis H test of several independent samples, the degree of mammary gland hyperplasia of rats in each group was $\chi^2 = 345.547$, $P = .000$. According to the level of $\alpha = .05$, the difference of hyperplasia degree of mammary gland tissue in each group was statistically significant.

Ras-GTP raises Raf kinase, which can activate and catalyze MEK after phosphorylation, and then cause ERK activation. Phosphorylated ERK enters the nucleus and activates the transcription of *c-jun*, *c-fos*, *c-myc*, and other transcription factors. Mammalian activator protein-1 (AP-1) is mainly composed of Jun and Fos families in the form of dimers. AP-1 is involved in cell growth, proliferation, apoptosis, differentiation, and other biological processes by combining DNA target sequence.²⁶ When Ras pathway is activated, miR-21 expression is up-regulated, and when AP-1 expression is inhibited by Fos inhibitor, miR-21 expression is significantly reduced. In the ER-Ras cell line, the expression level of miR-21 reaches the highest level at 48 to 72 hours after Ras activation, and the activity of

PDCD4 of target gene is almost inhibited. When AP-1 activity is inhibited, the expression of miR-21 is down-regulated and PDCD4 activity returned to the normal level. It was confirmed by dual-luciferase that there is AP-1 target in the 5'-flanking regulatory region of pri-miR-21.^{27,28} Interestingly, we used bioinformatics to predict that there was a binding site of miR-21 in the 3'UTR of Matrix metalloproteinase inhibitor-3 (TIMP-3) and reversion inducing cysteine rich protein with Kazal motifs (RECK). Then, the direct target relationship between miR-21 and TIMP-3 and RECK was confirmed by our dual-luciferase report. The RT-PCR and Western blot results also confirmed that miR-21 can negatively regulate the expression of TIMP-3 and RECK. As we all know, TIMP-3 is one of the members of

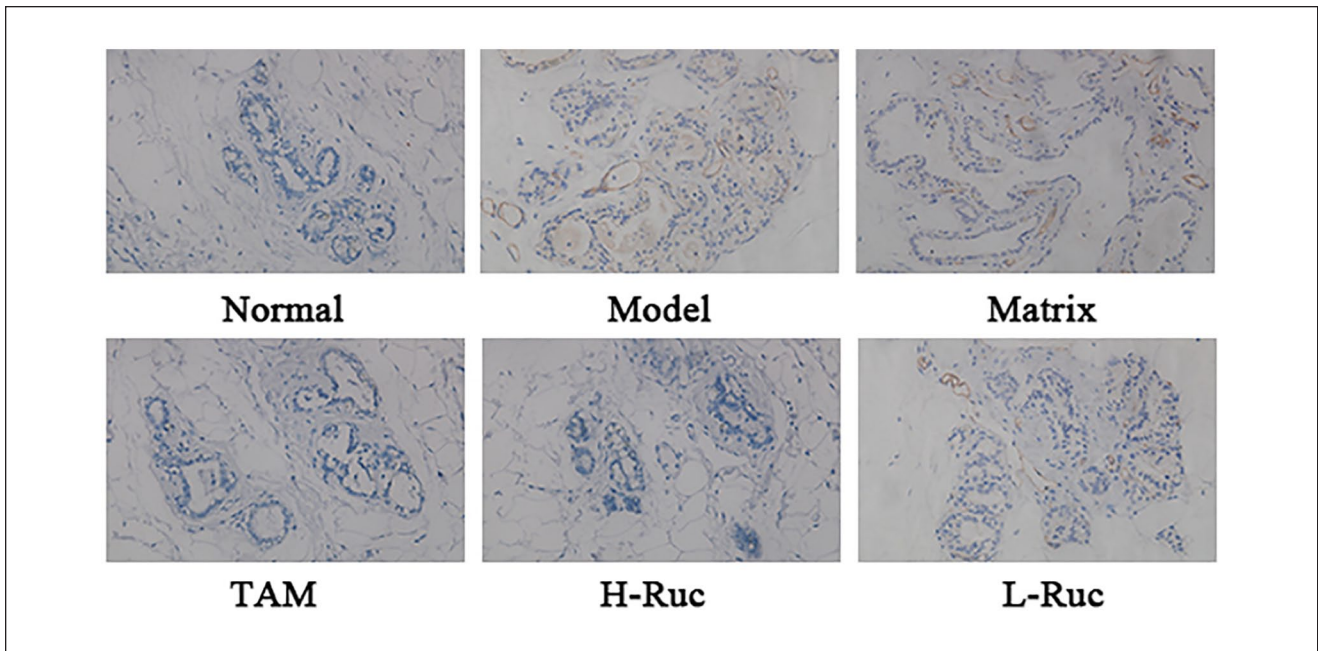


Figure 15. The vascular endothelial cell surface marker CD34 in breast precancerous lesions rats was determined by immunohistochemistry ($\times 200$ magnification).

the TIMPs family. Its biological function is mainly carried out by the N-terminal domain. The N-terminal domain of TIMP-3 is inserted into the crack-like active site of MMPs molecules to form a 1:1 MMP-TIMP complex, so as to inhibit the activity of MMPs, prevent ECM degradation and maintain tumor cell stability and inhibition of angiogenesis.²⁹ Takahashi et al³⁰ found RECK by cloning v-ki-ras gene into NIH3T3 fibroblasts. Human RECK is located on chromosome 9p12-13 and contains 13 single nucleotide polymorphisms (SNP), which can regulate 3 types of MMP (MMP-2, MMP-9, and MMP-14). The research showed that the negative regulation of RECK on MMP-9 might be through direct inhibition of MMP-9 enzyme activity or inhibition of extracellular secretion of MMP-9.³¹ And the inhibition of RECK on MMP-2 might be due to the inhibition of TIMPs, MT1-MMP, and pro-MMP-2 membrane anchored trisomic complex on the surface of cell membrane, preventing the maturation of pro-MMP-2. Furthermore, TIMPs could regulate RECK expression through the Rap1/Rac1 pathway, and ultimately participated in the downregulation of MMPs activity.³² This study showed that the RUt could inhibit Ras/Raf/MEK/ERK signal pathway, reduced AP-1 activity, down-regulated miR-21 expression, decreased the inhibition of miR-21 on TIMP-3 and RECK mRNA, promoted the expression of TIMP-3 and RECK protein and inhibited the expression of VEGF, MMP-2, and MMP-9 angiogenic protein, thus affecting the angiogenesis ability of MCF-10AT cells. Furthermore, by silencing H-Ras with siRNA, it was

found that RUc lost its inhibitory effect on the Ras/Raf/MEK/ERK signaling pathway; it could not inhibit AP-1 activity and reduce the expression of miR-21. And there was no significant difference in the expression of VEGF, MMP-2, MMP-9 angiogenic proteins compared with the control group (Figure 19).

The material basis and mechanism of action of traditional Chinese medicine are the focus of current research on traditional Chinese medicine. In our previous study,¹⁴ the HPLC-MS analysis result showed that RUc contains 15 main active components, including gallic acid, cyanidanol, chlorogenic acid, tetrahydropalmatine, rosmarinic acid, quercetin, luteolin, eugenol, kaempferol, apigenin, rhein, emodin, aloe emodin, 11 keto- β -boswellic acid, and 3-acetyl-11-keto- β -boswellic acid. These components can be divided into organic acids, tannins, alkaloids, volatile oil, anthraquinone, and flavonoids.¹⁴ Eugenol can down-regulate the c-Myc/PGC-1 β /ERR α signal pathway of MCF-10AT cells, inhibit oxidative phosphorylation (OXPHOS) and fatty acid oxidation (FAO), reduce oxidative stress of cells, and induce apoptosis and S-phase cell block through HER2/PI3K-Akt pathway and effectively reduce or inhibit breast precancerous lesions.^{15,16} Aloe emodin can induce apoptosis of MCF-10AT and MCF-7 cells by up-regulating miR-15a/miR-16-1 of Bcl-2.³³ Acetyl-11-keto- β -boswellic acid can inhibit the expression of ER- α protein through LINC00707/miR-206, thus promoting the apoptosis of MCF-10AT cells and inducing the cell cycle arrest of

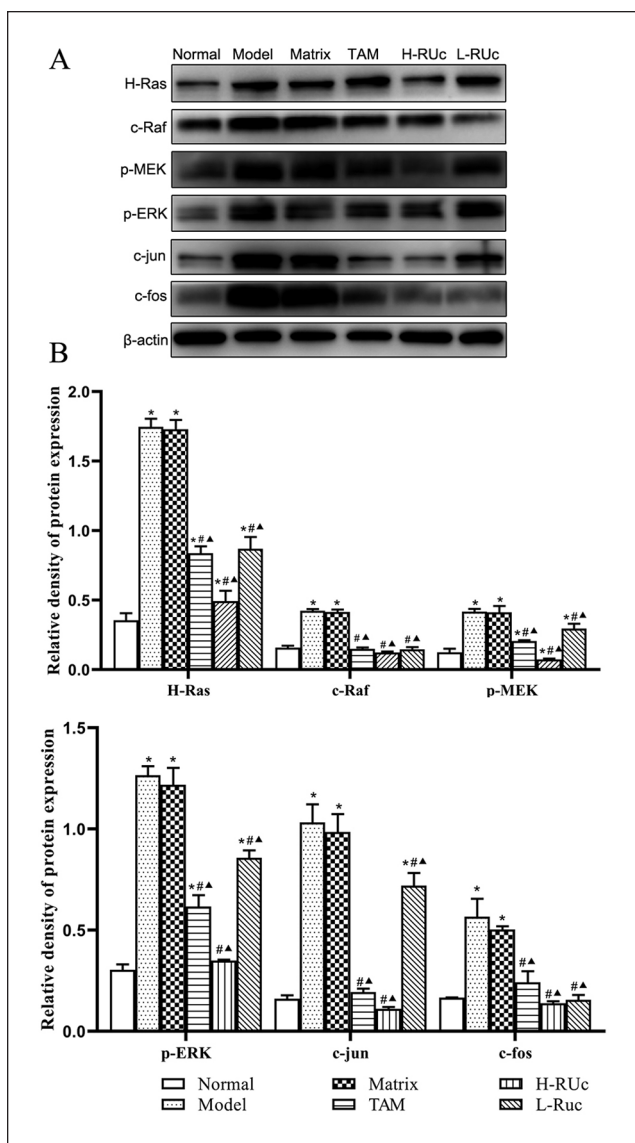


Figure 16. Effect of RUC on the regulation of the Ras/Raf/MEK/ERK signaling pathway in mammary tissue of rats with breast precancerous lesions. (A) Representative Western blot images of Ras/Raf/MEK/ERK signaling pathway related proteins in mammary tissue of rats. (B) The quantification of Ras/Raf/MEK/ERK signaling pathway related proteins levels.

* $P < .05$ versus Normal group. # $P < .05$ versus Model group. $\Delta P < .05$ versus Matrix group.

GO/G1 phase. Boswellic acid can be used as an effective anticancer drug, affecting angiogenesis (VEGF), inflammation (TNF- α , IL-12), apoptosis (caspase-3, caspase-9) and antioxidants (SOD and CAT), thus inhibiting the proliferation of MCF-7 cells and enhancing VEGF antibody induced cell death.³⁴ Quercetin inhibited calcineurin activity and calcineurin/nuclear transcription factor pathway, and inhibited angiogenesis of MCF-7 xenograft tumor in nude mice.³⁵ Rhein inhibited VEGF-stimulated

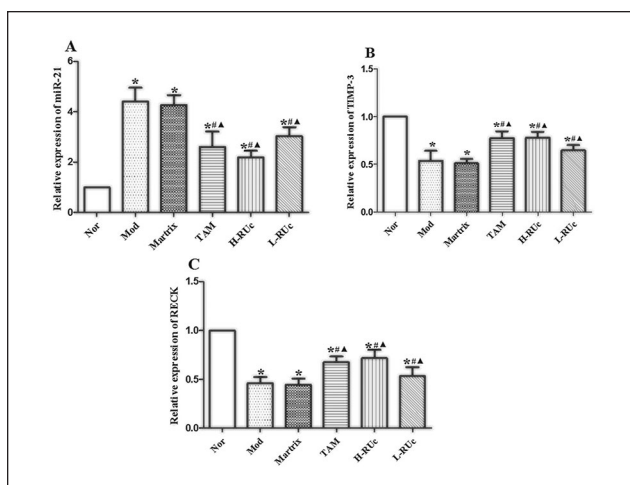


Figure 17. Effect of RUC on the expression of angiogenesis-associated genes miRNA21, TIMP-3 and RECK in mammary tissue of rats with breast precancerous lesions. (A) miRNA-21, (B) TIMP-3, (C) RECK. RT-PCR was used to analyze the expression levels of mRNA in mammary tissue of rats. Data are representative results of 3 independent experiments. * $P < .05$ versus Normal group. # $P < .05$ versus Model group. $\Delta P < .05$ versus Matrix group.

HUVECs proliferation, migration and tubular structure formation through PI3K/AKT/ERK signaling pathway under normoxia and hypoxia conditions, and inhibited hormone dependent (MCF-7) and non dependent (MDA-MB-435S) cell viability in a dose-dependent manner.³⁶ Kaempferol regulates VEGF/VEGFR2 and its downstream signal cascades (PI3K/AKT and MEK/ERK) by reducing the level of VEGFR-2 protein and kinase activity, and has an inhibitory effect on angiogenesis in HUVECs stimulated by VEGF.³⁷ Emodin can down-regulate the transcriptional activity of Runx2, inhibit the expression of MMPs and VEGFR-2 protein in breast cancer, and further inhibit tumor-induced metastasis and angiogenesis.³⁸ The above studies confirmed that many effective ingredients in RUC can promote the apoptosis of breast tumor cells, regulate energy metabolism and inhibit angiogenesis, thus inhibiting the proliferation of breast tumor cells. In this study, MCF-10AT cells were selected as the observation object to explore the effect of RUC on the angiogenesis of breast precancerous cells. The results showed that RUC could inhibit the proliferation of MCF-10AT cells, but had low cytotoxicity to HUVECs. It is worth noting that the conditioned medium of MCF-10AT cells treated with RUC could inhibit the proliferation, migration, invasion and tubular structure formation of HUVECs, and reduce the number of new capillaries in rat aortic rings. It is revealed that in the process of inhibiting angiogenesis, RUC might first act on MCF-10AT cells, rather than directly exert cytotoxic effects on HUVECs.

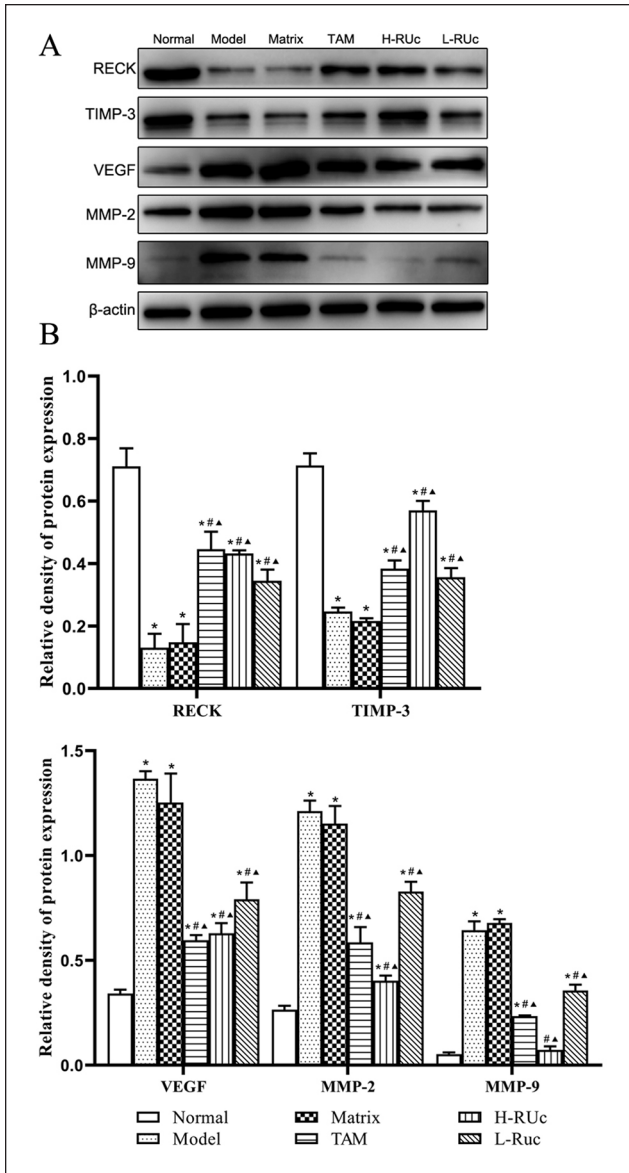


Figure 18. Effect of RUC on the regulation of the angiogenesis related proteins in mammary tissue of rats with breast precancerous lesions. (A) Representative Western blot images of RECK, TIMP-3, VEGF, MMP2, and MMP9 in mammary tissue of rats. (B) The quantification of angiogenesis related proteins levels.

*P < .05 versus Normal group; #P < .05 versus Model group; ▲P < .05 versus Matrix group.

In order to further verify the above inference, we established a rat model of breast precancerous lesions for in vivo experiments. It is noteworthy that the in vivo results also support the inference of in vitro cell experiments. After treatment with RUC, the microvessel density of rats with breast precancerous lesions decreased, and the related proteins of Ras/Raf/MEK/ERK signaling pathway, H-Ras,

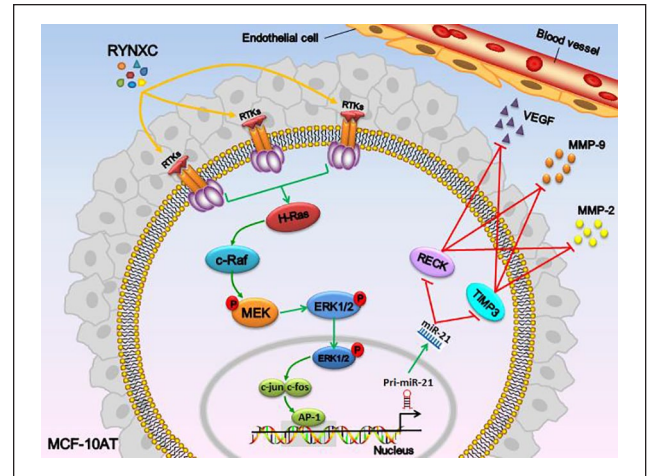


Figure 19. Mechanism of inhibitory Ras/Raf/MEK/ERK signaling pathway related proteins in MCF-10AT cells treated with RUC.

c-Raf, p-MEK, p-ERK, c-jun, and c-fos were inhibited. In addition, miR-21, VEGF, MMP2, and MMP9, the angiogenic genes, were also inhibited, while TIMP-3 and RECK. TIMP-3 and RECK were increased, and the trend of protein expression and gene was consistent.

Conclusion

In summary, the potential mechanism of angiogenesis in breast precancerous lesions may be closely related to the Ras/Raf/MEK-ERK signaling pathway. We found that RUC can inhibit the angiogenesis of breast precancerous lesions, which may be attributed to its inhibition of the Ras/Raf/MEK/ERK signaling pathway; it reduced the damage of miR-21 to TIMP3 and RECK, decreased the protein expression of VEGF, MMP2 and MMP9 and then suppressed the angiogenesis ability of endothelial cells.

Author’s Note

Guijuan Zhang is now affiliated to School of Nursing, Jinan University, Guangzhou, China.

Acknowledgments

The authors gratefully acknowledge TCGA for open access to their database.

Author Contributions

L.-S.J. and J.-X.J. conceived and designed the study. L.-S.J., J.-X.J. and Z. -G.J. performed the experiments, analyzed the data and wrote the manuscript. W.-J.Y., Q.-D, Y.-X.X., and L.-X.Y. assisted in performing the research. X.-X.Q. and M. -X.Y. provided language help and assisted in analyzing data. Y.-X.X. and M.-M. guided the whole research and provided financial support.

Declaration of Conflicting Interests

The author(s) declared no potential conflicts of interest with respect to the research, authorship, and/or publication of this article.

Funding

The author(s) disclosed receipt of the following financial support for the research, authorship, and/or publication of this article: This work was supported by the National Natural Science Foundation of China (No.82074430, 81803979, 81741130, 81673979, 81473688, and 81373314); the Natural Science Foundation of Guangdong Province, China (No.2018A030313393 and 2016A030313114); the general Project of Natural Science Foundation of Guangdong Province, China in 2022; Science and Technology Program of Guangzhou, China (No.201803010051, 201707010245, and 201704020117) and the Fourth Batch of TCM Clinical Outstanding Talent Program of China (No. 444258).

ORCID iD

Shujun Lin  <https://orcid.org/0000-0002-1589-7557>

Data Availability Statement

The data used in the current study are available from the corresponding author upon reasonable request.

References

- Bray F, Ferlay J, Soerjomataram I, Siegel RL, Torre LA, Jemal A. Global cancer statistics 2018: GLOBOCAN estimates of incidence and mortality worldwide for 36 cancers in 185 countries. *CA Cancer J Clin*. 2018;68:394-424.
- Feng X, Jing Z. Research progress of Chinese and western medicine in breast cancer precancerous lesions. *Med Inf*. 2015;28. doi:10.3969/j.issn.1006-1959.2015.47.603
- Dupont WD, Parl FF, Hartmann WH, et al. Breast cancer risk associated with proliferative breast disease and atypical hyperplasia. *Cancer*. 1993;71:1258-1265.
- Chen SS, Gu Y, Lu F, et al. Antiangiogenic effect of crocin on breast cancer cell MDA-MB-231. *J Thorac Dis*. 2019;11:4464-4473.
- Cui Y, Xu S, Gu Y, Zhang D, Zhang S. Effects of FGF-1 and FGFR1 on the genesis of spontaneous breast cancer in TA2 mice. *Chin J Clin Oncol*. 2009;36:168-171.
- Jin D, Yu X, Chen B, et al. Combined immunotherapy of breast cancer with EGF and VEGF vaccines from DNA shuffling in a mouse model. *Immunotherapy*. 2017;9:537-553. doi:10.2217/imt-2017-0004
- Bluff JE, Menakuru SR, Cross SS, et al. Angiogenesis is associated with the onset of hyperplasia in human ductal breast disease. *Br J Cancer*. 2009;101:666-672.
- Leach MO. Application of magnetic resonance imaging to angiogenesis in breast cancer. *Breast Cancer Res*. 2001;3:22-27.
- Hao Z, Zheng Y, Xiao G, Li S. Relationship between MAPK/ERK signaling pathway and tumor angiogenesis. *China Med Her*. 2015;12:148-151.
- Lee SJ, Namkoong S, Kim YM, et al. Fractalkine stimulates angiogenesis by activating the Raf-1/MEK/ERK- and PI3K/Akt/eNOS-dependent signal pathways. *Am J Physiol Heart Circ Physiol*. 2006;291:H2836-H2846.
- Sapino A, Goia M, Recupero D, Marchiò C. Current challenges for HER2 testing in diagnostic pathology: state of the art and controversial issues. *Front Oncol*. 2013;3:129.
- Hayes DF. HER2 and breast cancer - a phenomenal success story. *New Engl J Med*. 2019;381:1284-1286.
- Zhang S, Tang D, Guo X, Yin G. A research on angiogenic signaling pathways of anti-tumor therapies in Chinese Materia Medica(CMM). *World Sci Technol*. 2016;18:1827-1832.
- Chen R, Zhang G, Ma Y, Bie F, Fan H, Ma M. Pharmacodynamics and medicinal chemistry of an external Chinese herbal formula for mammary precancerous lesions. *Evid Based Complement Alternat Med*. 2017;2017:6235027.
- Ma M, Ma Y, Zhang GJ, et al. Eugenol alleviated breast precancerous lesions through HER2/PI3K-AKT pathway-induced cell apoptosis and S-phase arrest. *Oncotarget*. 2017;8:56296-56310.
- Yan X, Zhang G, Bie F, et al. Eugenol inhibits oxidative phosphorylation and fatty acid oxidation via downregulation of c-Myc/PGC-1 β /ERR α signaling pathway in MCF10A-ras cells. *Sci Rep*. 2017;7:12920.
- Liang S, Zhang G, Ma M, et al. Effect of topical Ruyanneixiao cream for VEGF and FGF2 expression in rat breast with mammary precancerous lesions. *J Jinan Univ*. 2015;36:484-489.
- Zhang PC, Liu X, Li MM, et al. AT-533, a novel Hsp90 inhibitor, inhibits breast cancer growth and HIF-1 α /VEGF/VEGFR-2-mediated angiogenesis in vitro and in vivo. *Biochem Pharmacol*. 2020;172:113771.
- Gucalp A, Traina TA, Eisner JR, et al. Male breast cancer: a disease distinct from female breast cancer. *Breast Cancer Res Treat*. 2019;173:37-48.
- Hoogerbrugge N, Bult P, de Widt-Levert LM, et al. High prevalence of premalignant lesions in prophylactically removed breasts from women at hereditary risk for breast cancer. *J Clin Oncol*. 2003;21:41-45.
- Page DL, Jensen RA, Simpson JF. Premalignant and malignant disease of the breast: the roles of the pathologist. *Mod Pathol*. 1998;11:120-128.
- Pilat MJ, Christman JK, Brooks SC. Characterization of the estrogen receptor transfected MCF10A breast cell line 139B6. *Breast Cancer Res Treat*. 1996;37:253-266.
- Dawson PJ, Wolman SR, Tait L, Heppner GH, Miller FR. MCF10AT: a model for the evolution of cancer from proliferative breast disease. *Am J Pathol*. 1996;148:313-319.
- Miller FR. Xenograft models of premalignant breast disease. *J Mammary Gland Biol Neoplasia*. 2000;5:379-391.
- Lu S, Jang H, Gu S, Zhang J, Nussinov R. Drugging Ras GTPase: a comprehensive mechanistic and signaling structural view. *Chem Soc Rev*. 2016;45:4929-4952.
- Zhou Y, Machius M, Nestler EJ, Rudenko G. Activator protein-1: redox switch controlling structure and DNA-binding. *Nucleic Acids Res*. 2017;45:11425-11436.
- Talotta F, Cimmino A, Matarazzo MR, et al. An autoregulatory loop mediated by miR-21 and PDCD4 controls the AP-1 activity in RAS transformation. *Oncogene*. 2009;28:73-84.
- Becker BLE, Yong L. Apoptosis and the target genes of microRNA-21. *Chin J Cancer*. 2011;30:371-380.

29. Rai GP, Baird SK. Tissue inhibitor of matrix metalloproteinase-3 has both anti-metastatic and anti-tumorigenic properties. *Clin Exp Metastasis*. 2020;37:69-76.
30. Takahashi C, Sheng Z, Horan TP, et al. Regulation of matrix metalloproteinase-9 and inhibition of tumor invasion by the membrane-anchored glycoprotein RECK. *Proc Natl Acad Sci U S A*. 1998;95:13221-13226.
31. Mendes SR, Amo-Maestro LD, Marino-Puertas L, Diego I, Goulas T, Gomis-Rüth FX. Analysis of the inhibiting activity of reversion-inducing cysteine-rich protein with Kazal motifs (RECK) on matrix metalloproteinases. *Sci Rep*. 2020;10:6317.
32. Oh J, Takahashi R, Kondo S, et al. The membrane-anchored MMP inhibitor RECK is a key regulator of extracellular matrix integrity and angiogenesis. *Cell*. 2001;107:789-800.
33. Jiang X, Liu Y, Zhang G, et al. Aloe-Emodin induces breast tumor cell apoptosis through upregulation of miR-15a/miR-16-1 that suppresses BCL2. *Evid Based Complement Alternat Med*. 2020;2020:5108298.
34. Saraswati S, Agrawal SS. Antiangiogenic and cytotoxic activity of boswellic acid on breast cancer MCF-7 cells. *Biomed Prev Nutr*. 2012;2:31-37.
35. Zhao X, Wang Q, Yang S, et al. Quercetin inhibits angiogenesis by targeting calcineurin in the xenograft model of human breast cancer. *Eur J Pharmacol*. 2016;781:60-68.
36. Fernand VE, Losso JN, Truax RE, et al. Rhein inhibits angiogenesis and the viability of hormone-dependent and -independent cancer cells under normoxic or hypoxic conditions in vitro. *Chem Biol Interact*. 2011;192:220-232.
37. Chin HK, Horng CT, Liu YS, et al. Kaempferol inhibits angiogenic ability by targeting VEGF receptor-2 and down-regulating the PI3K/AKT, MEK and ERK pathways in VEGF-stimulated human umbilical vein endothelial cells. *Oncol Rep*. 2018;39:2351-2357.
38. Ma J, Lu H, Wang S, et al. The anthraquinone derivative Emodin inhibits angiogenesis and metastasis through down-regulating Runx2 activity in breast cancer. *Int J Oncol*. 2015;46:1619-1628.